

Electrochemical Studies of Bitter Gourd (*Momordica charantia*) fruits as Ecofriendly Corrosion Inhibitor for Mild Steel in 1 M HCl Solution

Aijuan Zhao¹, Haijie Sun^{1,*}, Lingxia Chen¹, Yufang Huang¹, Xingjie Lu^{2,*}, Bing Mu¹, Hairong Gao¹, Shaoqing Wang¹, Ambrish Singh³

¹ Institute of Environmental and Catalytic Engineering, College of Chemistry and Chemical Engineering, Zhengzhou Normal University, Zhengzhou 450044, Henan, China.

² Henan Institute of Metrology, Zhengzhou-450000, Henan, China.

³ School of Materials Science and Engineering, Southwest Petroleum University, Chengdu, Sichuan 610500, China.

*E-mail: sunhaijie406@zznu.edu.cn, xingjieluzznu@163.com

Received: 9 March 2019 / Accepted: 22 April 2019 / Published: 10 June 2019

Fruits extract of *Momordica charantia* (MCFE) was characterized using gas chromatography (GC), and mass spectrometry (MS) methods. The influence of MCFE on corrosion of mild steel in 1M HCl solution was evaluated using static electrochemical methods. Electrochemical Impedance Spectroscopy (EIS) and polarization studies were performed to derive the kinetic mechanism taking place at the electrodes. Micro-electrochemical tests were performed using scanning electrochemical microscopy (SECM) technique. The surface was further examined by scanning electron microscope (SEM). The EIS results suggested that the increase in the concentration of MCFE increased the inhibition efficiency. Polarization statistics pointed towards the changes in the anodic and cathodic kinetics, but overall shift of $-E_{\text{corr}}$ was less than 85 mV suggesting the MCFE inhibitor belongs to mixed type category. SEM studies revealed that the surface of the mild steel was quite unaffected with MCFE film on it in 1M HCl solution.

Keywords: Mild steel; *Momordica charantia*; Corrosion; EIS; SECM; GC-MS

1. INTRODUCTION

Presence of scales, intermetallics, precipitates and debris inside the pipelines is a major blow to the oil companies as it reduces the production as well as the transportation. Acids in different volume are used to dissolve and clean these unwanted substances stuck to the pipelines. In the process of cleaning the pipes the acids do attack the pipelines and corrodes the metal surface. This can cause fatal injuries, accidents due to leakage and failure of the overall systems. Corrosion is a global problem and a lot of

money is being used to mitigate it. Almost all countries use 0.1-3% of their GDP in solving problems or finding replacements caused due to corrosion. Apart from the corrosive nature of the acids, pH and temperature also play a vibrant part in the evaluation of corrosion rate. Although, the mechanism of the formation and removal of the precipitates, intermetallics, debris and scaling is not entirely assumed due to the complicated reaction processes [1].

The literatures and available techniques suggests that still there is no method to control corrosion or to stop it completely. The process can be delayed with the use of several methods including, cathodic protection, galvanization, coating/spraying, and inhibitors. Inhibitors are chemical substances that are added to the system to mitigate corrosion. These substances adsorb on to the surface of the metal forming a film that keeps the corrosive media away from the metal. The use of inhibitors is one of the greatest technique used worldwide due to its low price, ease of usage, no requirement of special equipment's and availability [2-5]. Most of the inhibitors used are organic and their usage in higher concentrations are strictly forbidden by the environmental regulating authorities. As the higher concentration can affect the toxicity level and cause various problems. So, to keep these regulations and environment in front, use of ecofriendly inhibitors are in high demand. They are environment friendly, non-toxic and biodegradable that can be use in higher concentrations too. Many alkaloids, steroids, amines, fatty acids *etc.* are derived from plants which serve as an effective inhibitor. The heteroatoms (N, S, O), benzene ring, π -bonds presence in the inhibitors decide the potential and effectiveness of an inhibitor [6-10].

The inhibitor *Momordica charantia* used for the present study was selected for its recognized bitterness s shown in figure 1. It is also well-known as bitter melon, Okinawa, karavella (karela), balsam pear, bitter gourd or bitter squash. It is classified in the clan of Cucurbitaceae, and is broadly found in Asia, Africa, and the Caribbean for its edible fruit. Originally from India and was introduced to China later in the 14th century and now egg mixed with bitter gourd is a famous dish with the bitter melon tea in the mainland. The bitterness of the plant is due to the chemical substance Momordicin present in the fruit. The plant is rich in momordicin I, momordicin II, terpenoid compounds (including momordicin-28, momordicinin, momordicilin, momordenol, momordol), glycosides (including momordin, charantin, charantosides, goyaglycosides, momordicosides) and cucurbitacin B [11]. The regular use of the fruit can increase the beta cells in the pancreas which can further increase the insulin level thereby controlling Diabetes [12-16]. In contemporary research work we have investigated MCFE as corrosion mitigator of mild steel in HCl media through weight loss, electrochemical and surface studies.



Figure 1. *Momordica charantia* found in (a) India and (b) China.

2. EXPERIMENTAL

2.1. Grounding of inhibitor

The fruits of *Momordica charantia* were purchased from the vegetable market and were dehydrated in sun. 100 grams of desiccated *Momordica charantia* fruits were soaked in 900 ml of ethanol for 24 hours and refluxed for 5 hours. The extract was then mixed with reagent grade HCl and accumulated to 500 ml. The solution was further diluted to 25, 50, 100, 200 v/v (equivalent to 2%, 5%, 10% and 20% v/v wt. %) with HCl to prepare the four different concentrations of the inhibitor. The hostile solution of HCl (corrosion medium) was prepared by pure hydrochloric acid with double distilled water. The reagent grade HCl bottle was purchased from the chemical supplier in china. This solution was availed to elucidate the corrosion mitigation parameters.

2.2. Preparation of materials

Mild steel samples were mechanically abraded conferring to ASTM A262 standard and used for the corrosion study. The samples were washed repeatedly with H₂O and alcohol to remove any kind of adulteration and then dried at room temperature. The samples were covered with epoxy resin and left overnight to dry. As 1 cm² surface is required for the electrochemical studies. The samples were welded with copper wire and then placed in round utensil. This round utensil was filled with epoxy resin and left to dry overnight. Next day the sample with epoxy resin was (now round in shape due to round utensil) taken out and the bottom part was abraded continuously with different grades of emery paper (200, 400, 600, 800 and 1200). Once the bottom part of the mild steel (1 cm²) was seen clearly, it was then polished mechanically for a mirror finish.

2.3. Gas Chromatography (GC)

GC-2010 Plus machine by Shimadzu Japan was used to perform the gas chromatography tests. GC device was prepared with a single injector and two flame ionization detectors (FID). He (1 mL/min) was used as the carrier gas used in the process. Relative component concentrations were analyzed based on GC peak areas without using correction factors.

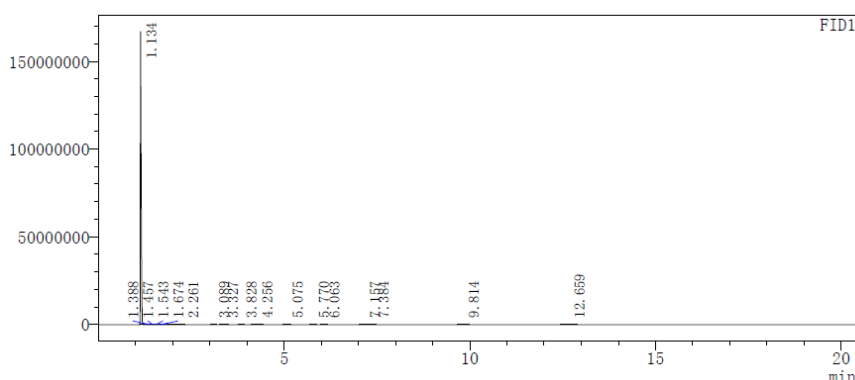
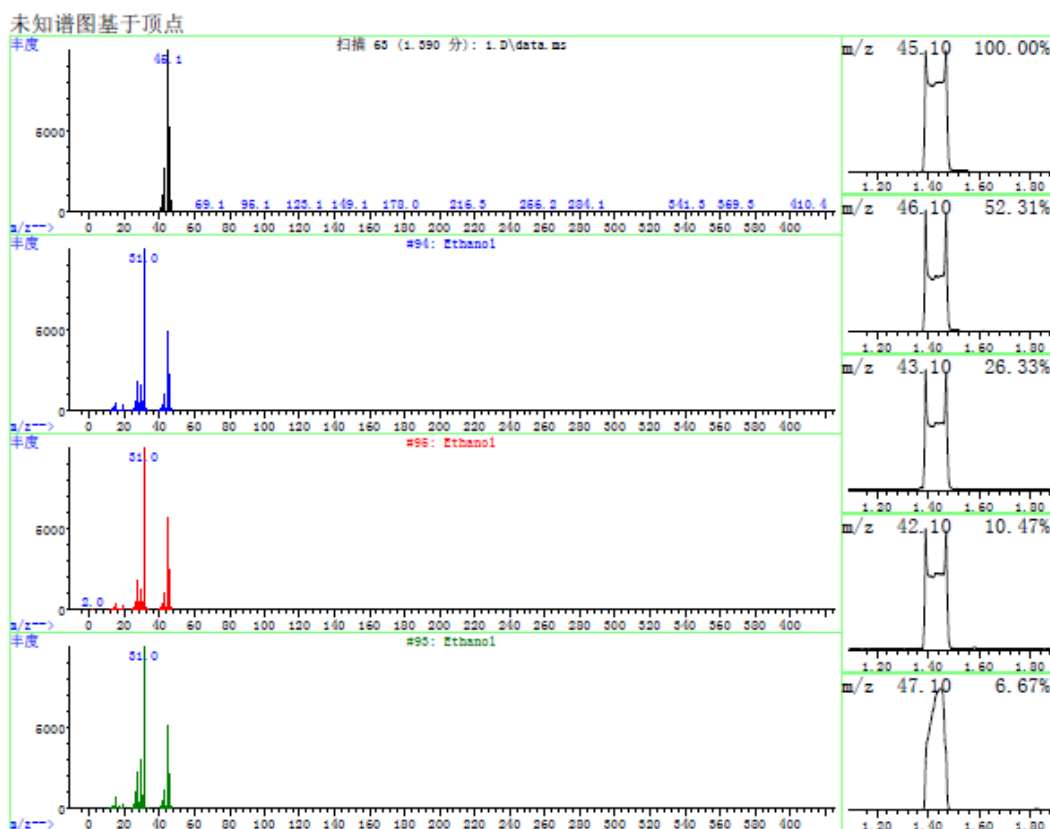


Figure 2. Gas chromatography peaks obtained for MCFE extract using flame ionization detector.

A number of noticeable peaks as shown in figure 2 were identified in the repeated GC investigations of the extract. Most of the peaks (1.388~1.674) are of terpenoids and similar to the already published work [17]. Among the peaks identified, they are very similar to Momordicin and other terpenoids [18].

2.4. Mass Spectrometry (MS)

GC7890-MS5975 (Agilent, USA) machine was used to perform the mass spectroscopy prepared with a HP-5MS capillary column (30 mm × 0.32 mm × 0.25 μm) and quadruple mass spectrometer. He (1 mL/min) was used as the carrier gas used in the process. Among the peaks identified, they are very similar to Momordicin, terpenoids and glycosides as shown in figure 3. The peaks obtained at 44.1, 66, 89, 119, correspond to the momordicin-28, momordicinin, momordicilin, momordenol terpenoids present in the fruit extract. Glycosides are lower in concentration so their peaks are at very intensity. All the peaks (Fig. 2) were matched in NIST library with their individual CAS number to get the exact information about the peaks [19].



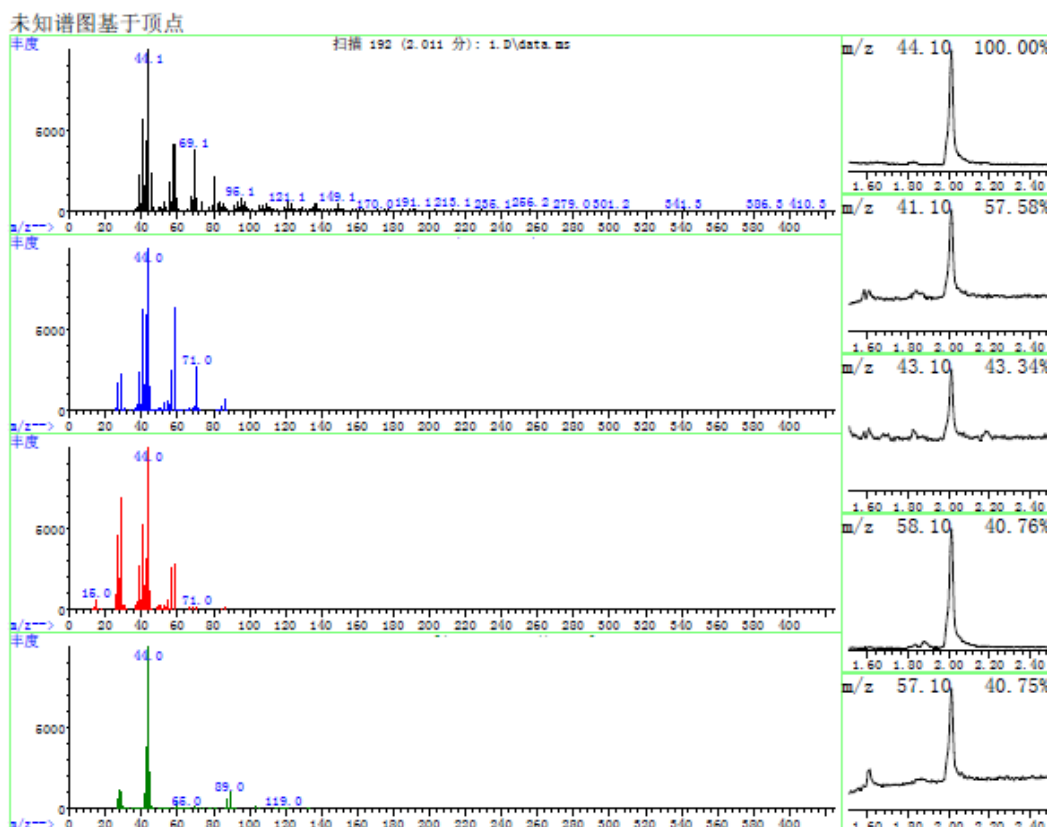


Figure 3. Mass spectrometry peaks of various components present in MCFE extract.

2.5. Electrochemical measurements

Three cell assembly of counter electrode, reference electrode and working electrode was employed to carry out the electrochemical tests on Autolab workstation. Nova and Zsimpwin softwares were used to analyze the obtained data. The tests were started after an immersion time of 30 minutes to ensure a stable potential. To attain this, an open circuit potential (OCP) test was performed for ~30 minutes vs. SCE to ensure the stable potential. The frequency ranges of 100 kHz to 10 mHz was selected to carry out all the electrochemical impedance spectroscopy (EIS) tests. The polarization tests were conducted at the potential of -250 mV to +250 mV with scan rate of 1 mV/s [20, 21].

Scanning electrochemical microscopy (SECM) was used to detect the localized changes on the metal surface using CHI900C workstation. The three cell electrode assembly was employed for the test but the size was much smaller than that used in the traditional electrochemical tests. The room temperature was maintained using the thermostat for all the experiments in absence and presence of inhibitors.

2.6. Scanning Electron Microscopy (SEM)

The mild steel surface was exposed to the ZEISS SEM instrument to determine the changes on the surface before and after corrosion. Different magnifications of 500x, 1000x and 2000x were used to

analyze the metal surface which was also shifted according to corroded and non-corroded regions. At room temperature the metal samples were immersed in the corrosive solution and left for 24 hours. The steel samples were further washed with water, and sodium bicarbonate solution. The samples were left to dry and kept in desiccator.

3. RESULTS AND DISCUSSION

3.1. Electrochemical measurements

3.1.1. Electrochemical Impedance Spectroscopy

The kinetics and the surface mechanism was studied using electrochemical impedance spectroscopy experiments. This method is one of the oldest and common method to determine the corrosion mitigation phenomenon [22, 23]. Open circuit potential (OCP) plots of the steel shows a stable corrosion potential as is evident by the figure 4a. One can observe a stable potential with a linear line for solution with and without inhibitor. This suggests that the time of 30 minutes was enough to attain a stable potential for the reaction. Figure 4b shows the Nyquist plots of mild steel in 1M HCl solution with and without MCFE solution.

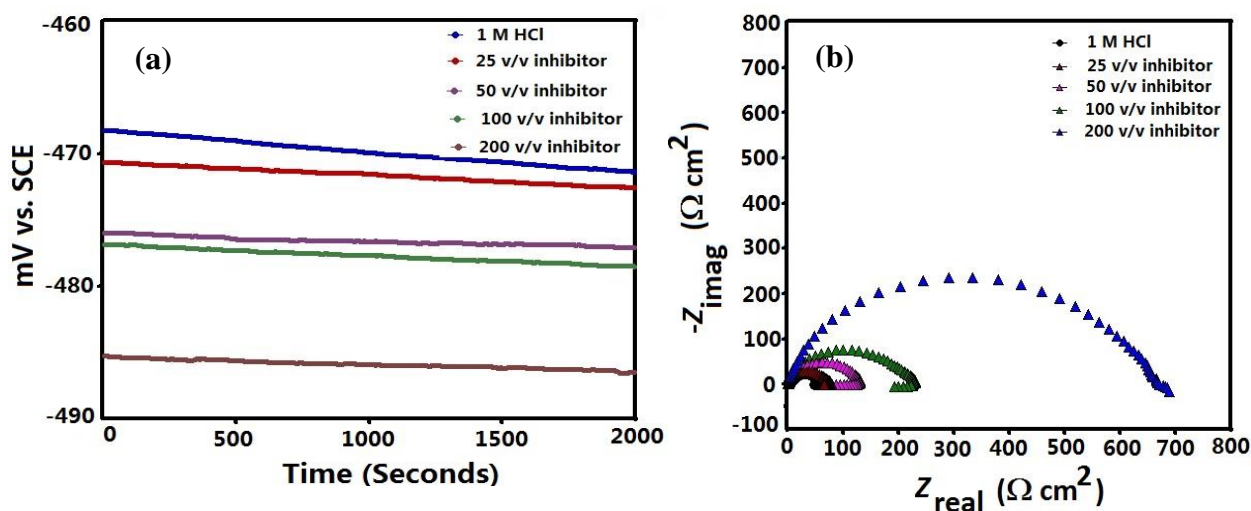


Figure 4. Electrochemical analyses for (a) OCP and (b) Nyquist plots for mild steel in absence and presence of MCFE at 10 mV amplitude.

The diameter of the Nyquist graphs increases with the addition of the inhibitor in the solution. And it goes bigger and bigger with the increase in inhibitor concentration. This is due to the increase in charge transfer resistance of the system. An inductive loop can be easily visualized in the Nyquist plots which suggests that the surface is non-homogeneous, rough and causing the dispersion effect to take place. The inductive loop in the lower frequency also results due to the stabilization phenomenon of the products formed during the corrosion process [24, 25].

The corresponding circuit was employed to fit the plots obtained from the impedance tests. The circuit is composed of R_s (resistance of solution), R_{ct} (charge transfer resistance), L , RL (inductive components) and the constant phase element (CPE) as depicted in figure 5.

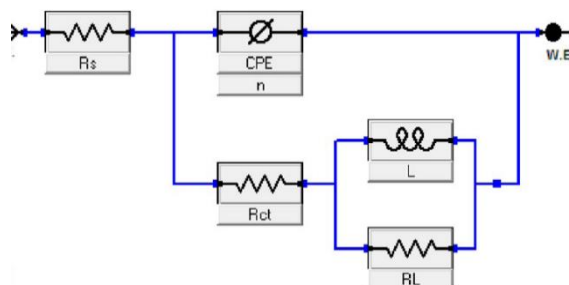


Figure 5. Equivalent circuit used to fit the Nyquist curves.

The inhibition efficiency is calculated using charge transfer resistance (R_{ct}) as follows,

$$\eta\% = \frac{R_{ct(inh)} - R_{ct}}{R_{ct(inh)}} \times 100 \tag{2}$$

Where $R_{ct(inh)}$ and R_{ct} are the values of charge transfer resistance with and without inhibitor in 1M HCl correspondingly. The R_{ct} values were seen to increase with the increase in inhibitor concentration. The values were less for the 1M HCl solution without inhibitor and with the addition of inhibitor in the solution the values tend to increase as shown in table 1. This increase in the values of R_{ct} may be due to the adsorption of inhibitor molecules on the metal surface and increase in the resistance [26-28].

Table 1. Nyquist data for mild steel in 1M HCl at diverse concentration of MCFE.

Solutions	Conc.(v/v)	R_s (Ω cm ²)	R_{ct} (Ω cm ²)	L	$\eta\%$
1 M HCl	-	1.2	25.4	-	-
MCFE	25	1.9	56.5	23	55
MCFE	50	2.4	110.6	18	77
MCFE	100	1.1	215.1	33	88
MCFE	200	1.9	644.6	-	96

3.1.2. Potentiodynamic polarization measurements

The polarization kinetics were extrapolated to obtain the corrosion current density (I_{corr}) and corrosion potential ($-E_{corr}$) values. The anodic (β_a) and cathodic (β_c) slopes were analysed by fitting the curves with the software to get the fitted data. The efficiency of the inhibitor was calculated using the equation below:

$$\eta\% = \frac{I_{corr} - I_{corr(i)}}{I_{corr}} \times 100 \tag{1}$$

where I_{corr} and $I_{\text{corr}(i)}$ are the corrosion current density with and without MCFE. The respective plots for mild steel with and without MCFE are presented in figure 6.

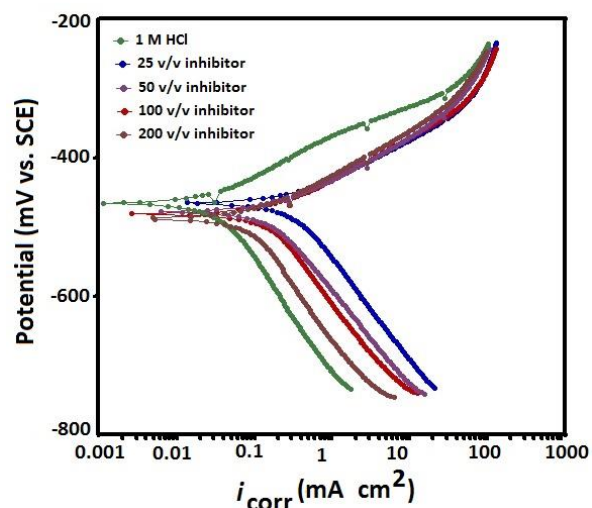


Figure 6. Potentiodynamic polarization plots for mild steel in absence and presence of MCFE at a scan rate of 1 mV/second.

An inference can be drawn from the figure that the anodic (b_a) and cathodic (b_c) polarization slopes were altered after the addition of the MCFE solution due to the reduction in anodic dissolution and suppression in hydrogen evolution reactions. The results also indicated the decrease in I_{corr} values in the presence of inhibitor due to the strong bonding between the inhibitor molecules and metal surfaces [29]. The overall corrosion rate also decreases in presence of MCFE and the inhibition efficiency increases gradually. However, the $-E_{\text{corr}}$ values were not much modified (less than 85 mV) as compared to the blank 1M HCl solution. This behaviour could be categorized in the mixed type category where the inhibitor is neither anodic nor cathodic [30]. Table 2 includes the value of all the obtained parameters such as the corrosion potential (E_{corr}), corrosion current density (I_{corr}), anodic (β_a) and cathodic (β_c) slopes [30].

Table 2. Potentiodynamic polarization data for mild steel in 1M HCl at different concentration of MCFE.

		Tafel data					
Solutions	Conc.(v/v)	E_{corr} (mV vs. SCE)	I_{corr} (mA cm ⁻²)	b_a (mV d ⁻¹)	b_c (mV d ⁻¹)	$\eta\%$ (%)	θ
1 M HCl	-	-465	326	61	160	-	-
MCFE	25	-468	136	63	194	58	0.58
MCFE	50	-475	105	61	165	68	0.68
MCFE	100	-477	30	63	148	89	0.89
MCFE	200	-486	21	62	196	94	0.94

3.1.3. Scanning Electrochemical Microscopy (SECM)

The micro-electrochemical techniques have proved their existence while being informative and resourceful for its operation on insulating and conducting metal surfaces [31]. These techniques can be used in variant modes to study the localized corrosion. The mild steel samples were cut in specified dimensions to fit in the CHI instrument to carry out the SECM experiments.

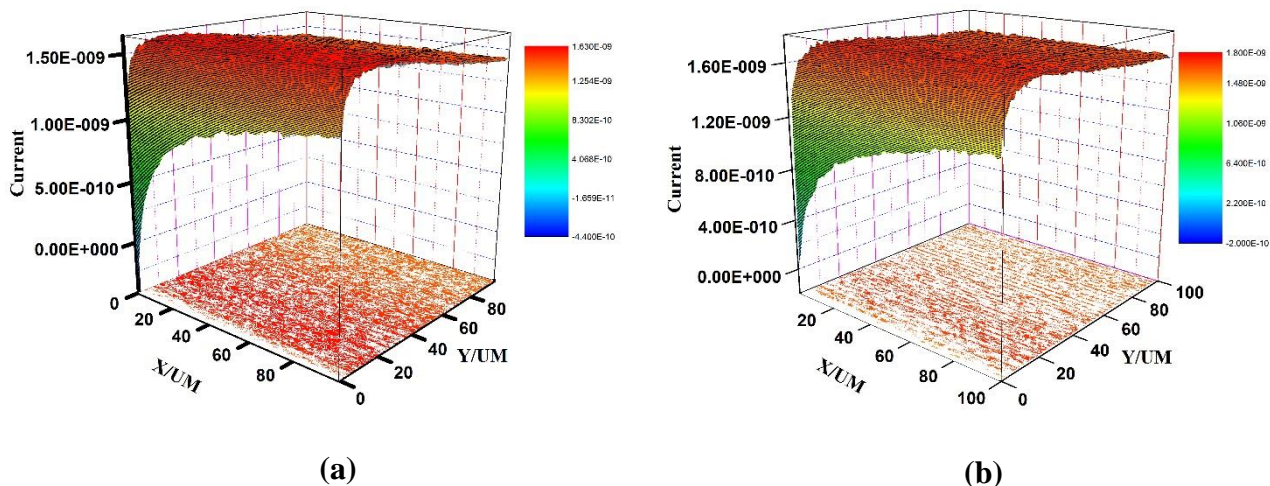


Figure 7. SECM 3D images for mild steel in 1M HCl and 1M HCl + MCFE.

The cell was assembled with three electrode system and a platinum probe was used to vibrate over the metal surface to receive the information on corrosion reactions. The probe was established at an equi-distance over the mild steel surface using the probe approach curve mode before the start of each test [32]. Figure 7, b shows the 3D picture of the scan done through SECM mode by the instrument. The mild steel surface was observed to act as conductor in absence of the inhibitor as this is evident from the figure where the current was higher as the steel was in direct contact with the probe. While, when the metal surface intact with inhibitor film was exposed to the vibrating probe, the current observed was lower due to the non-contact between metal surface and the probe. This observation was due to the insulating action of the metal covered with inhibitor film. After comparing the currents of metal surface with and without inhibitor film the protective action of the inhibitor could be verified [33].

3.3. Surface Morphology Tests

3.3.1. Scanning Electron Microscopy (SEM)

The mild steel samples were washed with sodium bicarbonate mixture trailed by acetone, then dehydrated and retained in desiccator prior to their exposure to SEM tests [34]. The samples were then taken to the Zeiss Tescan instrument to conduct the tests of the surface to get high resolution micrographs through SEM. The samples were also sprayed with gold for better conductivity of the surface and to get high quality figures. Figure 8a shows the morphology of the mild steel that is very irregular and non-uniform without inhibitor. While with inhibitor film present, the surface of mild steel is even, regular

and unbroken as shown in figure 8b. So, the mild steel surface was smooth in presence of MCFE and irregular without it [35].

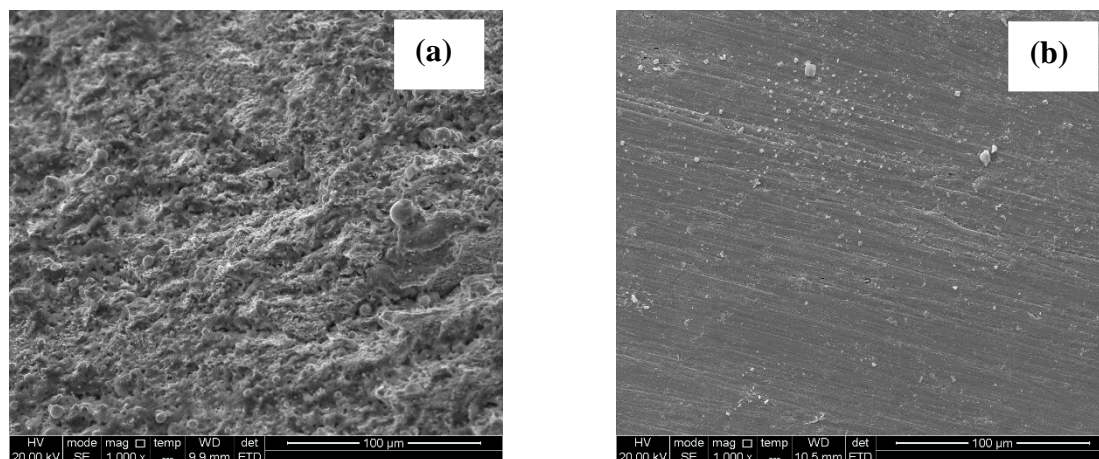


Figure 8. SEM pictures for mild steel in (a) 1M HCl and (b) 1M HCl + MCFE.

3.4. Mechanism of adsorption and inhibition

The process of adsorption relies mainly on the structure of the inhibitor, charge, and dissemination of the inhibitor molecule over the steel surface [36]. The adsorption is a complicated process as it involves various factors accounting for it. So, it is very difficult to assume a single adsorption process especially for a plant (fruit, leaves, stem, flower, seed etc.) extract. The presence of several chemical constituents in an extract makes it impossible to determine or establish the single mode of adsorption [37]. The chemical constituents inhibit the metal due to their synergistic effect and crediting one constituent out of several is very difficult. The presence of momordicin, terpenoids, glycosides etc. in the current MCFE solution also make it difficult to establish the mode of adsorption. So, in general an establishment can be made on the basis of experimental results that the synergistic effect between the chemical constituents of the MCFE solution can successfully mitigate the corrosion reaction of the mild steel by covering the entire metal surface [38, 39]. The whole surface gets covered by the MCFE molecules forming a film that does not allow the penetration of aggressive acidic media onto the steel surface. All the active centres on the steel surface that take part in the corrosion reaction were covered or blocked by the MCFE molecules. This phenomenon is evidently proved by all the experimental results where the efficiency can be seen increasing with MCFE solution [40-43].

5. CONCLUSIONS

- The electrochemical and surface examinations of the MCFE inhibitor indicated that it can be used for mitigating the corrosion of mild steel in 1M HCl solution.
- The increase in the diameter of the Nyquist plots with addition of MCFE inhibitor indicated the increase in resistance which further pointed towards the increase in the efficiency of inhibition.

- The kinetics of the polarization curves was found to be affected in both the anodic and cathodic region. But, overall shift in any particular direction could not be seen with $-E_{\text{corr}}$ values with 85 mV. All these circumstances pointed that the MCFE can be included into the group of mixed type inhibitor.
- The scanning electrochemical microscopy also revealed that the surface acted as insulator with MCFE film on it and as conductor without the inhibitor film.
- The scanning electron microscopy showed the irregular steel surface without MCFE film on it and smooth and even surface with MCFE film on the steel.

ACKNOWLEDGEMENTS

This work was supported by the Key Scientific and Technological Project of Henan Province (192102210139), the Key Scientific Research Project of Henan Province (18A180018), the Environmental Catalysis Innovative Research Team of Zhengzhou Normal University (702010), and the Student Innovative Program of Zhengzhou Normal University (DCZ2017014).

References

1. A. Singh, K.R. Ansari, J. Haque, P. Dohare, H. Lgaz, R. Salghi, M.A. Quraishi, *J. Taiwan Inst. Chem. E.*, 82 (2018) 233.
2. Hongwei Feng, A. Singh, Yuanpeng Wu, Yuanhua Lin, *New. J. Chem.*, 42 (2018) 11404.
3. Ambrish Singh, E.E. Ebenso, M. A. Quraishi, *Int. J. Electrochem. Sci.* 7 (2012) 3409.
4. M. A. Quraishi, A. Singh, V. K. Singh, D. K. Yadav, A.K. Singh, *Mater. Chem Phys.* 122(2010) 114.
5. Ambrish Singh, I. Ahamad, V. K. Singh, M. A. Quraishi, *J. Solid State Electr.* 15 (2011) 1087.
6. S. Chen, A. Singh, Yuanluqi Wang, Wanying Liu, Kuanhai Deng, Yuanhua Lin, *Int. J. Electrochem. Sci.*, 12 (2017) 782.
7. Haolong Yang, Ming Zhang, A. Singh, *Int. J. Electrochem. Sci.*, 13 (2018) 9131.
8. A. Singh, E. E. Ebenso, M. A. Quraishi, Y. Lin, *Int. J. Electrochem. Sci.*, 9 (2014) 7495.
9. A. Singh, K. R. Ansari, X. Xu, Z. Sun, A. Kumar, Y. Lin, *Sci. Report.*, 7 (2017) 14904
10. Hongqiang Wan, Peiyong Han, Shuai Ge, Fancong Li, Simiao Zhang, Huan Li, A. Singh, *Int. J. Electrochem. Sci.*, 13 (2018) 9302.
11. Ambrish Singh, Yuanhua Lin, Wanying Liu, Eno E. Ebenso, Jie Pan, , *Int. J. Electrochem. Sci.*, 8 (2013) 12884.
12. Toshihiro; Akihisa, Naoki; Higo, Harukuni; Tokuda, Motohiko; Ukiya, Hiroyuki; Akazawa, Yuichi; Tochigi, Yumiko; Kimura, Takashi Suzuki, *J. Natur. Pds.* 70 (2007) 1233.
13. A. Singh, I. Ahamad, M. A. Quraishi, *Arab. J. Chem.*, 9 (2016) S1584.
14. S. Sharma, S. Tandon, B. Semwal, K. Singh, *J. Pharm. Res. Opin.* 1 (2011) 42.
15. He Chen, shuaiqi Zhang, Zhixue Zhao, Meng Liu, Qingrui Zhang, *Proc. Chem.*, 31 (2019) 572.
16. A. Singh, K. R. Ansari, A. Kumar, W. Liu, C. Songsong, Yuanhua Lin, *J. Alloys Comp.*, 712 (2017) 121.
17. He Gao, Jia-Jia Wen, Jie-Lun Hu, Qi-Xing Nie, Hai-Hong Chen, Shao-Ping Nie, Tao Xiong, Ming-Yong Xie, *Food Biosci.*, 29 (2019) 62.
18. Li-Jie Zhang, Chia-Ching Liaw, Ping-Chun Hsiao, Hui-Chi Huang, Ming-Jen Lin, Zhi-Hu Lin, Feng-Lin Hsu, Yao-Haur Kuo, *J. Funct. Foods.*, 6 (2 0 1 4) 5 6 4.
19. O. Kenny, T.J. Smyth, C.M. Hewage, N.P. Brunton, *Food Chem.*, 141 (2013) 4295.
20. A. Singh, Y. Lin, W. Liu, E. E. Ebenso, J. Pan, *Int. J. Electrochem. Sci.*, 8 (2013) 12884.

21. Yuanhua Lin, Ambrish Singh, E. E. Ebenso, Yuanpeng Wu, Chunyang Zhu, H. Zhu, *J. Tai. Inst. Chem. Eng.*, 46 (2015) 214.
22. Priyanka Singh, A. Singh, M.A. Quraishi, *J. Taiwan Inst. Chem. E.*, 60 (2016) 588.
23. Wang Xiaohong, Peng Zhengwei, Ma Lai, *Int. J. Electrochem. Sci.*, 12 (2017) 11006.
24. Xihua Xu, A. Singh, Z. Sun, K. R. Ansari, Y. Lin, *R. Soc. Open Sci.*, 4 (2017) 170933.
25. Ambrish Singh, Eno E. Ebenso, M.A. Quraishi, *Int. J. Electrochem. Sci.* 7 (2012) 4766.
26. A. Singh, K. R. Ansari, M. A. Quraishi, Hassane Lgaz, Yuanhua Lin, *J. Alloys Comp.*, 762 (2018) 347.
27. A. Singh, Y. Lin, I. B. Obot, E. E. Ebenso, *J. Mol. Liq.*, 219 (2016) 865.
28. Ambrish Singh, Y. Lin, I. B. Obot, E. E. Ebenso, K. R. Ansari, M. A. Quraishi, *Appl. Surf. Sci.*, 356 (2015) 341.
29. A. Singh, Yuanhua Lin, K. R. Ansari, M. A. Quraishi, E. E. Ebenso, Songsong Chen, W. Liu, *Appl. Surf. Sci.*, 359 (2015) 331.
30. Ambrish Singh, Y. Lin, W. Liu, S. Yu, J. Pan, C. Ren, D. Kuanhai, *J. Ind. Eng. Chem.*, 20 (2014) 4276.
31. D. K. Yadav M. A. Quraishi, *Ind. Eng. Chem. Res.* 51 (2012) 14966.
32. S. Deng, X. Li, *Corros. Sci.* 55 (2012) 407.
33. A. J. Bard, F. R. F. Fan, J. Kwak, O. Lev, *Anal. Chem.* 61 (1989) 132.
34. C. Lee, J. Kwak, A. J. Bard, *Proc. Natl. Acad. Sci. USA*, 87 (1990) 1740.
35. S. Amemiya, Z. Ding, J. Zhou, A. J. Bard, *J. Electroanal. Chem.* 7 (2000) 483.
36. Chitrasen Gupta, Ishtiaque Ahamad, A. Singh, Xihua Xu, Zhipeng Sun, Yuanhua Lin, *Int. J. Electrochem. Sci.*, 12 (2017) 6379.
37. A. Singh, Y. Lin, Chunyang Zhu, Y. Wu, E. E. Ebenso, *Chin. J. Pol. Sci.*, 33 (2015) 339.
38. A. Singh, Neetesh Soni, Yu Deyuan, Ashish Kumar, *Res. Phys.*, 13 (2019) 102116.
39. Ambrish Singh, K.R. Ansari, Yuanhua Lin, M.A. Quraishi, Hassane Lgaz, Ill-Min Chung, *J. Taiwan Inst. Chem. E.*, 95 (2019) 341.
40. A. Singh, Yin Caihong, Yang Yaocheng, Neetesh Soni, Yuanpeng Wu, Yuanhua Lin, *ACS Omega*, 4 (2019) 3420.
41. Ambrish Singh, Mohd Talha, Xihua Xu, Zhipeng Sun, and Yuanhua Lin, *ACS Omega*, 2 (2017) 8177.
42. Ambrish Singh, Yuanhua Lin, Eno. E. Ebenso, Wanying Liu, Jie Pan, Bo Huang, *J. Ind. Eng. Chem.*, 24 (2015) 219.
43. Xiaohong Wang, Zhengwei Peng, Shiyu Zhong, *Int. J. Electrochem. Sci.*, 13 (2018) 8970.